TRANSITION FROM MIXED TO FORCED CONVECTION FOR OPPOSING VERTICAL FLOWS IN LIQUID-SATURATED POROUS MEDIA

SAND--85-0270C

DE85 010662

Daniel C. Reda
Fluid and Thermal Sciences Department
Sandia National Laboratories
Albuquerque, NM 87185

submitted for presentation
International Symposium on Geothermal Energy
August 26-30, 1985
Kailua-Kona, Hawaii

DISTRIBUTION OF THIS DOCUMENT IS UNLIMITED

DISCLAIMER

DISCLAIMER

TRANSITION FROM MIXED TO FORCED CONVECTION FOR OPPOSING VERTICAL FLOWS IN LIQUID-SATURATED POROUS MEDIA

Daniel C. Reda

Sandia National Laboratories, Albuquerque, NM 87185

ABSTRACT

Mixed-convection phenomena can occur within liquid-dominated geothermal reservoirs due to interactions of injected flows, or ground-water flows, with the buoyancy-induced fluid motion. This problem was studied experimentally and numerically for the case of opposing flows about a vertical heat source in a liquid-saturated porous medium. The ratio of the Rayleigh number (Ra) to the Peclet number (Pe) was identified as the nondimensional parameter which characterizes the relative influence of buoyancy-driven to pressure-gradient-driven fluid motion. The transition from mixed to forced convection was numerically determined to be (Ra/Pe) ≈ -0.5, where the minus sign denotes superimposed downflow. Agreement between measured and predicted thermal-field results showed that the finite-element code of Gartling and Hickox [1982 a,b] can be used to model low-temperature (single-phase) geothermal reservoirs throughout the natural, mixed, and forced convection regimes.

INTRODUCTION

A recent assessment of low-temperature geothermal energy resources presented by Sorey [1982] shows that significant quantities of usable energy reside in hydrothermal convection systems. In these liquid-dominated geothermal systems, buoyancy-driven water motion occurs in the vicinity of high heat flux regions. In some cases, these high heat flux regions may be vertical, e.g., the magmatic intrusions discussed by Cheng [1976].

The potential occurrence of mixed-convection phenomena in liquid-dominated geothermal reservoirs has been discussed by Cheng [1977], O'Sullivan [1980], and Morgan [1981]. Superimposed flows through geothermal reservoirs can result from two sources: natural and/or man-made. In the first case, subsurface ground-water flows interact with the buoyancy-driven fluid motion. In the second case, cold water may be injected into the reservoir in order to maintain production pressure, reducing the extent of local boiling near the production well, and thus increasing the useful life of the liquid-dominated reservoir.

In the present research, an experimental and numerical study was conducted to address the problem of mixed convection in liquid-saturated porous media. Buoyancy-driven upflow was induced about a cylindrical heat source immersed vertically in a uniform liquid-saturated porous medium; this natural-convection state was then systematically perturbed by the superposition of pressure-gradient-driven flows which opposed the buoyancy-induced liquid motion. The Reynolds number based on the superimposed pore velocity and the average particle size remained always less than unity to ensure the applicability of Darcy's law.

Attention is focused in this paper on defining the transition from the mixed- to the forced-convection regime.

EXPERIMENTAL APPROACH

A schematic of the axisymmetric test vessel is shown in Figure 1. The vertical annular region containing the liquid-saturated porous medium had a radial gap width $\Delta r = 20.96$ cm, and was bounded by an inner cylinder of radius $r_i = 0.95$ cm and a concentric outer cylinder of radius $r_o = 21.91$ cm. The inner cylinder was comprised of a finite-length heat source, supported above and below by insulating sections. Power input to the heater was held constant at P = 198.8 W/m over a heated length $1.9 \leq Z/\Delta r \leq 3.1$. The overlying liquid layer, and the outer circumference of the test region, were both maintained isothermal at 21.5°C.

Superimposed downflows within the porous medium were created by introducing pressurized water (at 21.5°C) into the overlying liquid layer through injection ports located in the upper boundary, while simultaneously withdrawing water from the medium through screen-covered bleed holes distributed across the lower boundary. Superimposed upflows were created by reversing

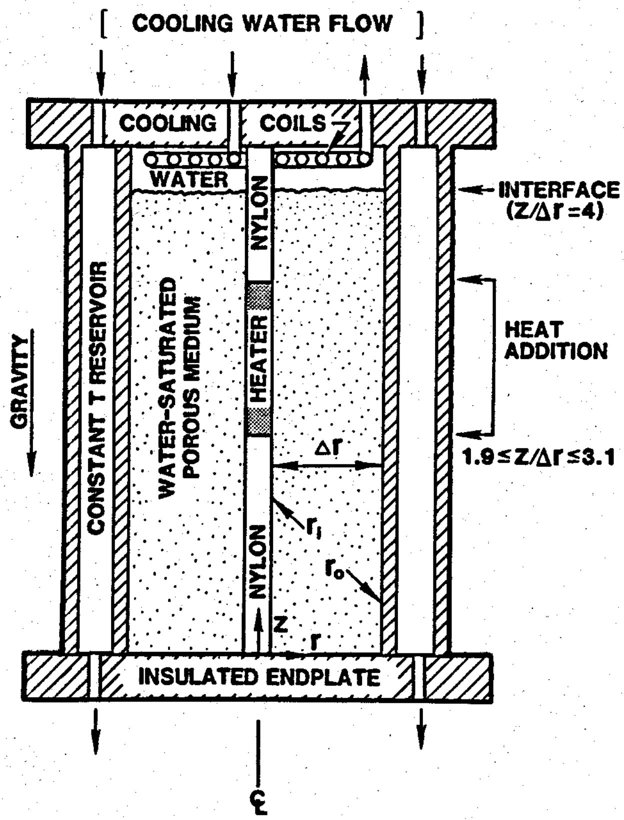

Figure 1. Schematic of Apparatus

this procedure. The volumetric flow rate was maintained constant for each test; measurements of this parameter yielded a value for the average superimposed pore velocity, $\overline{V}_p$ (where negative values for $\overline{V}_p$ denote downflow). The porous medium was comprised of glass beads, essentially spherical, with the following measured properties: average diameter, $\overline{d} = 650\mu m$; porosity, $\phi = 0.34$; permeability, $k = 611 \times 10^{-12} m^2$; and liquid-saturated thermal conductivity, $K_e = 0.87$ W/m-°C.

The two dimensionless parameters which characterize the present problem are the Rayleigh number, $Ra = (\rho_f g \beta_f \Delta T k r_i / \mu_f \alpha_e)$, which quantifies the potential for buoyancy-driven liquid motion, and the Peclet number, $Pe = (\overline{V}_p r_i / \alpha_e)$, which quantifies the influence of the superimposed flow. Here, ρ_f is fluid density, g is the gravitational constant, β_f is the volumetric expansion coefficient for the liquid, ΔT is the difference between the average heater surface temperature and the outer boundary temperature, μ_f is fluid viscosity, and α_e is thermal diffusivity of the liquid-saturated medium. If Ra and Pe are based on the same length scale (e.g., r_i) then the ratio (Ra/Pe) can be used to characterize the relative influence of buoyancy-driven to pressure-gradient-driven fluid motion. As this ratio becomes large, natural convection dominates. As this ratio approaches zero, forced convection dominates. Mixed convection occurs in the intermediate regime, where (Ra/Pe) is of order one.

Transient and steady-state natural convection experiments were conducted with this apparatus by Reda [1984]; Ra, based on r_i, was measured to be 7.25 for P = 198.8W/m. In the present work, $\overline{V}_p$ was varied from −391 to +233 μm/s, yielding a Pe range of −17.9 to +10.7 and a range for the ratio (Ra/Pe) of −0.41 to +0.68. The maximum value for the Reynolds number $[\rho_f \mid \overline{V}_p, max \mid \overline{d}/\mu_f]$ was 0.26, assuring the existence of Darcy flow under all test conditions. In the present paper, we focus attention on the case of superimposed downflow.

THEORETICAL APPROACH

The finite-element code of Gartling and Hickox [1982 a,b] was used in the present effort. This code, called MARIAH, utilizes Darcy's law as the momentum equation. The porous matrix is assumed to be rigid and in thermal equilibrium with the fluid. Density changes are allowed to occur in the fluid solely in response to changes in temperature. In accordance with the traditional Boussinesq approximation, the effects of such density changes are accounted for in the buoyancy term in the equations of motion and are neglected elsewhere. The fluid is treated as Newtonian, and the effects of viscous dissipation of energy are neglected. Thermal-dispersion effects, spatially dependent permeabilities, and temperature-dependent properties for the liquid can all be modeled. Two-dimensional geometries, in both rectangular and axisymmetric coordinates, can be treated.

RESULTS

Figures 2 and 3 show numerically predicted streamlines and isotherms for several $\overline{V}_p \leq 0$ cases. (These plots are meant to provide visual overviews and relative comparisons, hence individual contours are not labeled; quantitative comparisons of predictions and measurements will be given in subsequent figures.) Note first the natural convection results (for $\overline{V}_p = 0$). As a result of the constant-pressure, permeable-surface boundary condition imposed across the upper surface, essentially all of the streamlines were predicted to be U-shaped; i.e., fluid exited from the porous medium near the inner cylinder in a region of buoyancy-driven upflow, while an equal mass flux of fluid entered the porous medium near the outer boundary in a region of downflow. Isotherms showed that the thermal energy input to the liquid-saturated porous medium

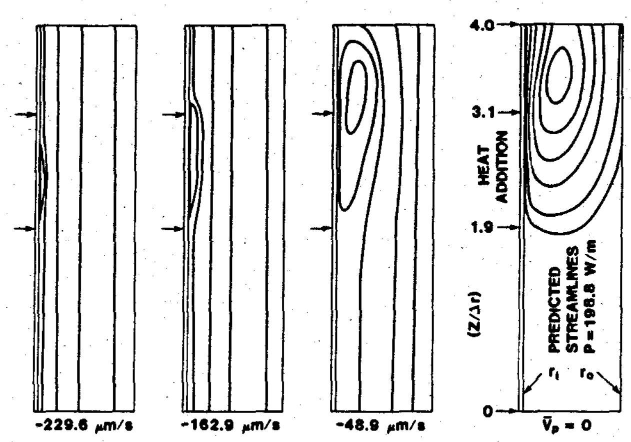

Figure 2. Predicted Streamlines as a Function of $\overline{V}_p$

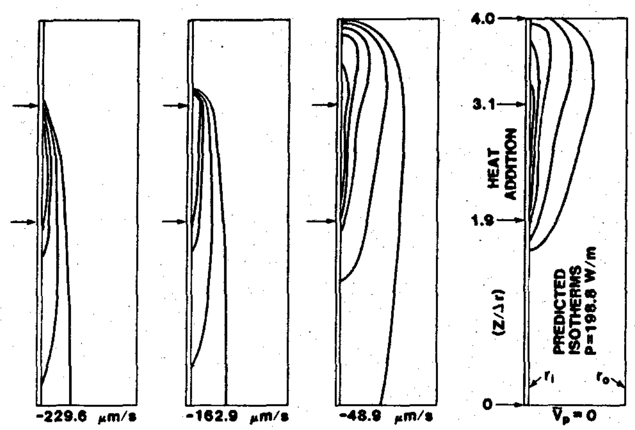

Figure 3. Predicted Isotherms as a Function of $\overline{V}_p$

was convected upward along the inner cylinder boundary. Temperatures of the porous medium adjusted to match that of the overlying liquid layer in the immediate vicinity of the permeable interface. Minor temperature increases occurred immediately below the heat addition region due to conduction heat transfer within the inner cylinder materials (an effect accounted for in the solution procedure).

Consider now the evolution of the mixed-convection velocity and thermal fields. As the strength of the superimposed downflow was increased, the buoyancy-induced upflow along the inner boundary was at first retarded, then stagnated, and ultimately suppressed. As a result, a closed, recirculating-flow region, or cell, was seen to form, decreasing in physical size as the downflow Peclet number was increased. For those cases where a closed cell (bounded on one side by r_i) was predicted to exist, the downflow streamline along the r_i boundary was predicted to "separate" from this boundary at the uppermost extent of the cell and "reattach" to this same boundary at the lower extent of the cell. In other words, the local pore velocity along the r_i boundary was predicted to change direction at each of two locations, upflow occurring along r_i between reattachment and separation, with downflow along r_i at all other locations. Predicted cell occurrence and predicted cell height (distance between separation and reattachment) thus provided information which could be used to quantify the (Ra/Pe) limit for the transition from mixed to forced convection.

Predicted isotherms showed that the natural convection of thermal energy in an upward direction changed to a forced convection of thermal energy in a downward direction as $|\overline{V}_p|$ was systematically increased. The relationship between predicted cell height and the corresponding thermal field (both measured and predicted) will be explored later in this section.

Figure 4 shows measured and predicted temperatures (T_i) along the r_i boundary, at each of four vertical locations, as a function of superimposed flow conditions. For $\overline{V}_p > 0$, at all measurement stations adjacent to and above the heated region, T_i values monotonically decreased from natural convection values as Pe was systematically increased from zero, consistent with the increased convective cooling of a constant-heat-flux source. For superimposed downflows, as the magnitude of the Peclet number was increased, T_i values above, and adjacent to, the heat source initially increased, reached maximum values, then decreased. To better interpret these downflow results, we focus attention initially on the $Z/\Delta r = 3.5$ measurement station (above the heat source) then progress sequentially downward in the direction of the superimposed flow to other measurement locations.

For $Z/\Delta r = 3.5$, T_i steadily increased above its natural convection value as |Pe| was increased from zero to ≈ 4, indicating a steadily increasing retarda-

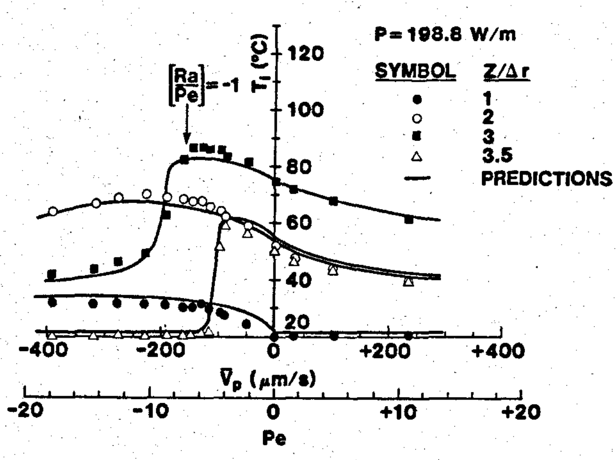

Figure 4. Inner Cylinder Surface Temperatures as a Function of $\overline{V}_p$

tion of the thermally driven upflow along the r_i boundary. A maximum T_i value was reached at this location for $|\mathrm{Pe}| \approx 4$, at which point a small additional increase in $|\mathrm{Pe}|$ caused an abrupt reduction in T_i to a temperature equal to that of the injected liquid. This response is clearly indicative of local upflow stagnation at this elevation, followed by a suppression of the upflow stagnation point to some elevation below $Z/\Delta r = 3.5$. The attainment of a maximum T_i value at any elevation above the heat source could thus potentially serve as an indicator of downflow separation from the r_i boundary. (This point will be discussed in more detail with Figure 6.)

Similar T_i versus Pe responses were observed at the $Z/\Delta r = 3.0$ and 2.0 locations, the attainment of the maximum T_i state occurring at progressively higher $|\mathrm{Pe}|$ values as the $Z/\Delta r$ elevation under scrutiny was lowered. Temperatures near the top and bottom of the heat source "crossed over" just after the (Ra/Pe) = -1 condition was reached, indicating downflow along some, or all, of the heat addition region. The T_i value at $Z/\Delta r = 1$ rose above the ambient level for all Pe < 0 states, indicating the formation of a thermal wake downstream of the heat-addition region. As can be seen in Figure 4, numerically predicted results were found to be in good agreement with measured values over the complete $\overline{V}_p$ range investigated, thereby corroborating the overall picture of upflow retardation, stagnation, and cell suppression given by the streamlines and isotherms of Figures 2 and 3.

Figure 5 further expands on the results of Figure 4. Here we see a plot of the vertical temperature difference along the heated surface,

$$\Delta T_z = T_i \text{ (at } Z/\Delta r = 3) - T_i \text{ (at } Z/\Delta r = 2)$$

as a function of the superimposed average pore velocity. For $\overline{V}_p \geq 0$, ΔT_z was positive, reaching a maximum measured value of + 24°C for weak superimposed upflow, where (Ra/Pe)$\approx$ 5. For $\overline{V}_p < 0$, ΔT_z steadily decreased as $|\overline{V}_p|$ was increased. A rapid crossover from positive to negative values occurred just after the (Ra/Pe) = -1 condition was reached. A maximum negative value for ΔT_z of -23°C was measured for (Ra/Pe)≈ -0.5, essentially equal and opposite to the maximum upflow ΔT_z value of + 24°C.

It should be noted that this measured (and predicted) trend for ΔT_z as a function of average superimposed pore velocity implies that the thermal response of a buried, finite-length, constant-heat-flux source could potentially be used to measure groundwater motion. Similar observations, based on analytic results, were reported by Romero [1983].

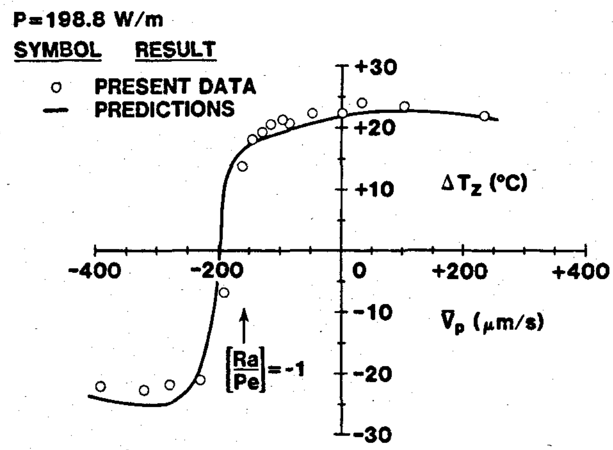

Figure 5. Vertical Temperature Difference Along Heated Surface as a Function of $\overline{V}_p$

In Figure 6 we show the loci of predicted separation and reattachment point locations along the r_i boundary as a function of the superimposed downflow pore velocity. The vertical extent of the heat addition region, wherein P = 198.8 W/m, is shown for reference. Also shown is the locus of predicted maximum T_i "states", or values, in comparison with measured data. Each pairing of a $\overline{V}_p$ value and a $Z/\Delta r$ elevation on this T_i locus corresponds to the attainment of the maximum T_i condition, at that particular elevation, as $\overline{V}_p$ was varied from zero to minus infinity (see again Figure 4).

Let us focus attention initially on the computed velocity field results. Three flow regimes, labeled I, II, and III, were found to exist. In the first regime,

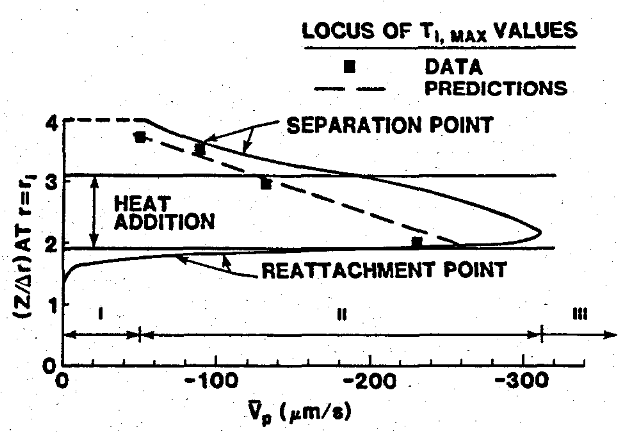

I: $-\infty \leq$ Ra/Pe<-3.17; STREAMLINE AT r_i REACHES INTERFACE.
II: $-3.17 \leq$ Ra/Pe < -0.51; CLOSED CELL BOUNDED BY r_i EXISTS WITHIN POROUS MEDIUM.
III: $-0.51 \leq$ Ra/Pe < 0 ; ONLY DOWNFLOW EXISTS.

Figure 6. Cell Height as a Function of $\overline{V}_p$; Definition of Flow Regimes

bounded by conditions $-\infty \leq$Ra/Pe< -3.17, the upflow streamline along the r_i boundary reached the permeable interface at $Z/\Delta r = 4$, hence no separation point existed on the r_i boundary. Reattachment of a downflow streamline to the r_i boundary did occur everywhere within this regime, even for the natural convection case. In the limit of Pe = 0, a very weak counter-rotating cell (not shown in Figure 2) was predicted to form below the heat addition region. In the second regime, given by $-3.17 \leq$ Ra/Pe< -0.51, the upflow streamline along the r_i boundary stagnated somewhere below the permeable interface. In this regime, both a separation and a reattachment point were predicted to exist, i.e., a trapped, recirculating-flow region was predicted to form immediately adjacent to this inner boundary. Throughout this regime, as |Pe| was increased, the vertical distance between separation and reattachment was predicted to decrease. For (Ra/Pe) $= -1$, predicted separation and reattachment point locations approached the top, and bottom, of the heat addition region, respectively. Cell height approached zero, at the $Z/\Delta r = 2.15$ location, as (Ra/Pe) approached a value of -0.51. In the third regime, given by $-0.51 \leq$ Ra/Pe < 0, only downflow was predicted to exist within the porous medium.

Interpreting these results in terms of the transition from natural to mixed convection is not straightforward. For opposing flows, mixed convection could be reasoned to exist throughout regime II and well into regime I. No precise definition of this transition, in terms of a limiting (Ra/Pe) value, can be given. Predicted cell disappearance, however, provides a clear demarcation of the transition from mixed to forced convection, in the limit as (Ra/Pe) approaches ≈ -0.5.

Additional numerical calculations, for P = 119.3 and 278.3 W/m, were then undertaken. Results showed that the (Ra/Pe) "boundary" between flow regimes I and II was dependent on heat flux. Predicted cell height, however, was found to consistently shrink to match the vertical extent and location of the heat-addition region whenever the ratio (Ra/Pe) approached ≈ -1, independent of heat flux. Similarly, the transition from mixed to forced convection, as defined by predicted cell disappearance, always occurred under flow conditions where the ratio (Ra/Pe) approached ≈ -0.5, independent of heat flux. Utilization of this ratio to characterize the relative influence of buoyancy-induced to pressure-gradient-driven motion in liquid-saturated porous media was thus validated.

The only other investigator to offer a quantitative definition for the transition from mixed to forced convection in liquid-saturated porous media was Cheng [1977]. Based on predicted heat transfer rates, obtained from similarity solutions for opposing flows about inclined surfaces, Cheng defined this transition in terms of a limiting Grashof-to-Reynolds number ratio (both dimensionless parameters based on an identical length scale); the limiting value of this ratio was found to be 0.15. It can be shown that Cheng's ratio of dimensionless parameters is identical to the (Ra/Pe) ratio invoked herein. Hence, the magnitude of Cheng's analytically derived limit (for a planar, inclined surface) is found to be consistent with the magnitude of the numerically generated limit (for a vertical, cylindrical surface) presented here.

We now focus attention on the $T_{i,max}$ locus of Figure 6 in an attempt to relate the thermal and velocity field results. Two general observations were made. First, this locus of $T_{i,max}$ states was predicted to be a linear function of $\overline{V}_p$, showing decreasing elevations as the magnitude of the superimposed pore velocity was increased, in good agreement with measured results. Second, this locus fell everywhere within the predicted recirculating-flow region, but its location relative to the predicted separation and reattachment points was strongly dependent on the ratio of predicted cell height to heated length.

Expanding on this last point, we note that two distinct situations occurred within flow regime II. For any given $\overline{V}_p$ value which resulted in the predicted separation point being well above the heat addition region (cell height greater than heated length), the attainment of the $T_{i,max}$ condition was found to occur at an elevation just below separation. Hence, for such cases, measurement of the $T_{i,max}$ state could serve as a reasonable indicator of upflow stagnation, and thus mean downflow separation.

On the contrary, for any given $\overline{V}_p$ value which resulted in the predicted separation point being adjacent to the heat-addition region (cell height less than heated length), attainment of the $T_{i,max}$ condition no longer occurred at an elevation in close proximity to separation. In fact, as $|\overline{V}_p|$ was increased, and the vertical dimension of the cell was reduced to an extent less than that of the heat-addition region, the attainment of the $T_{i,max}$ state (for each $\overline{V}_p$ value) was seen to shift from the top to the bottom of the cell. In such cases, measurement of the $T_{i,max}$ state would not be a valid indicator of mean downflow separation. Reexamination of the streamline and isotherm patterns corresponding to the $\overline{V}_p = -229\mu$m/s case of Figures 2 and 3 helps to illustrate this point. When separation occurred below the top of the heat-addition region, some portion of the total thermal energy dissipated in the heater was input to the superimposed downflow. This downflow subsequently separated from, then reattached to, the r_i boundary. Redeposition of thermal energy near the reattachment point thus forced local temperature levels to increase.

In summary, combined experimental and numerical results presented herein serve to illustrate the complex fluid-mechanic phenomena which can occur in hydrothermal convection systems subjected to superimposed flows.

CONCLUSIONS

1. Based on numerically predicted results, the transition from mixed to forced convection for vertically opposing flows in liquid-saturated porous media occurs for $(Ra/Pe) \approx -0.5$.

2. Combined experimental and numerical results show that the thermal response of a buried, finite-length, constant-heat-flux body could conceivably be used to measure groundwater motion.

3. Based on comparisons of measured and predicted thermal-field results, the finite-element code of Gartling and Hickox [1982 a,b] offers a viable computational approach to the modeling of two-dimensional, liquid-saturated geothermal reservoirs.

ACKNOWLEDGEMENTS

This work was performed at Sandia National Laboratories supported by the U. S. Department of Energy under contract number DE-AC04-76DP00789.

REFERENCES

Cheng, P., 1976, "Buoyancy Induced Boundary Layer Flows in Geothermal Reservoirs," Proc. 2nd Workshop on Geothermal Reservoir Engineering, Stanford University, pp. 236-246.

Cheng, P., 1977, "Combined Free and Forced Convection Flow about Inclined Surfaces in Porous Media," Int. J. Heat Mass Transfer, Vol. 20, pp. 807-814.

Gartling, D. K., and Hickox, C. E., 1982a, "MARIAH - A Finite Element Computer Program for Incompressible Porous Flow Problems, Part I - Theoretical Background," Sandia National Laboratories, Technical Report SAND79-1622.

Gartling, D. K., and Hickox, C. E., 1982b, "MARIAH - A Finite Element Computer Program for Incompressible Porous Flow Problems: User's Manual," Sandia National Laboratories, Technical Report SAND79-1623 (Revised).

Morgan, P., Harder, V., Swanberg, C. A., and Daggett, P. H., 1981, "A Groundwater Convection Model for Rio Grande Rift Geothermal Resources," Geothermal Resources Council, TRANSACTIONS, Vol. 5, pp. 193-196.

O'Sullivan, M. J. and Pruess, K., 1980, "Numerical Studies of the Energy Sweep in Five-Spot Geothermal Production/Injection Systems," Proc. 6th Workshop on Geothermal Reservoir Engineering, Stanford University, pp. 204-212.

Reda, D. C., 1984, "Natural Convection Experiments About a Finite-Length Cylindrical Heat Source in a Liquid-Saturated Porous Medium," Paper No. 16h, Proceedings AIChE Annual Meeting, San Francisco, CA.

Romero, L. A., 1983, "Low Peclet Number Convection Past a Spheroid in a Saturated Porous Medium," Sandia National Laboratories, Technical Report SAND83-0291.

Sorey, M. L., Reed, M. J., Mariner, R. H., and Nathenson, M., 1982, "Assessment of Low-Temperature Geothermal Resources in the United States," Geothermal Resources Council, TRANSACTIONS, Vol. 6, pp. 479-482.